Available online at www.sciencedirect.com
ScienceDirect
Estuarine, Coastal and Shelf Science 78 (2008) 426–436
ESTUARINE COASTAL AND SHELF SCIENCE
www.elsevier.com/locate/ecss

Uncertainty of excess density and settling velocity of mud flocs derived from in situ measurements

Michael Fettweis

Management Unit of the North Sea Mathematical Models (MUMM), Royal Belgian Institute of Natural Sciences, Gulledelle 100, 1200 Brussels, Belgium

Received 27 November 2007; accepted 14 January 2008
Available online 25 January 2008

Abstract

Direct or indirect measurements of excess density and settling velocity are inherently associated with uncertainties (errors) due to a lack of accuracy of the measuring instruments, inadequate precision of the observations, and the statistical nature of the variables (floc size, primary particle size and primary particle density). When using observations, some understanding of the uncertainties is needed. Based on the theory of error propagation, we have estimated the error of the excess density and the settling velocity of mud flocs using the measurement data of OBS, SPM filtration, LISST 100C, CTD and Sedigraph. The measurements were carried out between 2003 and 2005 in the southern North Sea in the course of eight tidal cycles. The excess density was calculated based on fractal description of mud flocs and using floc and water density data. The water density was derived from CTD measurements and the floc density was calculated using SPM concentration, particle volume concentration, and water and primary particle densities. The settling velocities of flocs were calculated on the basis of their fractal structure following Winterwerp, J. [1998. A simple model for turbulence induced flocculation of cohesive sediments. Journal of Hydraulic Research 36, 309–326].

The results show that the relative standard deviations for excess density, fractal dimension and settling velocity are about 10%, 2.5% and 100%, respectively. These uncertainties should be regarded as lower limits of the real error because the errors due to inaccuracies of the OBS, LISST and Sedigraph have been excluded, as they are unknown. From the results it was found that the statistical error of excess density was dominated by uncertainties of SPM concentration and primary particle density, and for fall velocity by uncertainties of primary particle and floc sizes, respectively. These statistical uncertainties will always be high when dealing with natural flocs or particles and cannot be reduced by increasing the accuracy of the instruments. They should therefore be taken into account when modelling cohesive sediment transport, either by using the calculated standard deviations for settling velocity, or by introducing a floc size (settling velocity) distribution in the transport model.

Keywords: settling velocity; floc density; error propagation; flocs; North Sea

1. Introduction

Knowledge on cohesive sediment transport processes is required to predict the distribution of suspended and deposited cohesive sediments in natural or anthropogenically created environments such as navigation channels and harbours. Settling of mud flocs is controlled by flocculation and hence also determines the transport of cohesive sediments. Flocculation/deflocculation is the process of floc formation and break-up which has a direct impact on settling velocity. The settling velocity is a function of the particle size and excess (also called effective) density, and can be described by Stokes' Law under the assumption that the particle Reynolds number is smaller than one. However, because the Suspended Particulate Matter (SPM) consists of a population of flocs with heterogeneous sizes, densities, and shapes (e.g. Eisma and Kalf, 1987; van Leussen, 1994), the settling velocity of mud flocs in natural environments will vary and, in the case of very large particles, could therefore depart from Stokes' Law. Measuring the floc settling velocity is hampered by technical limitations owing to their size and resistance against shear stresses, properties,

E-mail address: m.fettweis@mumm.ac.be

0272-7714/$ - see front matter © 2008 Elsevier Ltd. All rights reserved.
doi:10.1016/j.ecss.2008.01.007

which may be altered if flocs are taken out of the environment where they were formed. Furthermore, experimental observations are always subject to uncertainties that can be typically attributed to random measurement errors (lack of precision), systematic errors (lack of accuracy), human error, and intrinsic variable stochasticity. Within the field of flocculation of cohesive sediment dynamics, stochastic uncertainty is of primary importance, as recently recognised in the studies of Lee and Matsoukas (2000), Jackson (2005), Khelifa and Hill (2006), and Maggi (2007) who studied the fluctuations of the average and median floc size over time. When using experimental results, some understanding of the uncertainties in such results is also needed.

Two different methods exist for sampling settling velocity: direct and indirect ones. Direct methods are typically carried out in situ (or even in the lab). For this purpose, a number of different techniques have been developed (Owen tube, Griffith tube, LISST-ST, photo cameras, video systems), see, e.g., Dyer et al. (1996) and Eisma et al. (1996). The LISST 100 (Laser In-Situ Scattering and Transmissometer) has become a standard measuring instrument for particle size spectra and volume concentrations for applications in sea and estuarine waters (e.g. Agrawal and Pottsmith, 2000; Gartner et al., 2001; Mikkelsen and Pejrup, 2001; Fugate and Friederichs, 2002; Chang et al., 2006; Fettweis et al., 2006; Curran et al., 2007). However, neither the excess density nor the settling velocity can be directly measured by this instrument; Mikkelsen and Pejrup (2001) have presented an indirect method to calculate the settling velocity based on LISST 100 results together with SPM concentration measurements. The main advantage of this method is that it is convenient to use, but up to now it is not known what the error is of this indirect (or even direct) method is. The objective of our study therefore, is to apply a similar indirect method to calculate the excess density and the settling velocity using measured data of OBS, SPM filtration, LISST 100, CTD, and grain size analysis, and then to estimate the accuracy of excess density and settling velocity. Studies of uncertainties are often limited by calculating the sensitivity of parameters; in our case error propagation theory has been applied on all measured data in order to estimate the total uncertainty on excess density and settling velocity.

2. Methods

2.1. Regional settings

The measurements described here have been carried out in the southern North Sea, more specifically in the Belgian nearshore zone (Fig. 1). The area is characterised by depths between 5 and 35 m, a mean tidal range at Zeebrugge of 4.3 m (2.8 m) at spring (neap) tide and by maximum current velocities of more than 1 m/s. The winds are mainly from the southwest and the highest waves occur during north-westerly winds. The area is of interest due to the occurrence of a highly turbid coastal zone. The SPM concentration measurements indicate variation between a minimum of 20–70 mg/l and a maximum of 100–1000 mg/l; lower values (<10 mg/l) have been measured in the offshore area. The source of the SPM is mainly the inflowing water entering the area through the Dover Strait (Fettweis et al., 2007b). The SPM concentration measurements indicated variations between approximately 50 and 1000 mg/l; lower values (<10 mg/l) were measured offshore.

2.2. Tidal measurements

The field data were collected from the R/V Belgica during eight tidal cycles between February 2003 until July 2005; the vessel was moored to maintain the position during the tidal cycle (see Table 1 and Fig. 1). The measurements were carried out in the coastal turbidity maximum (MOW1, B&W Oostende) and further offshore (Kwintebank, Hinderbank).

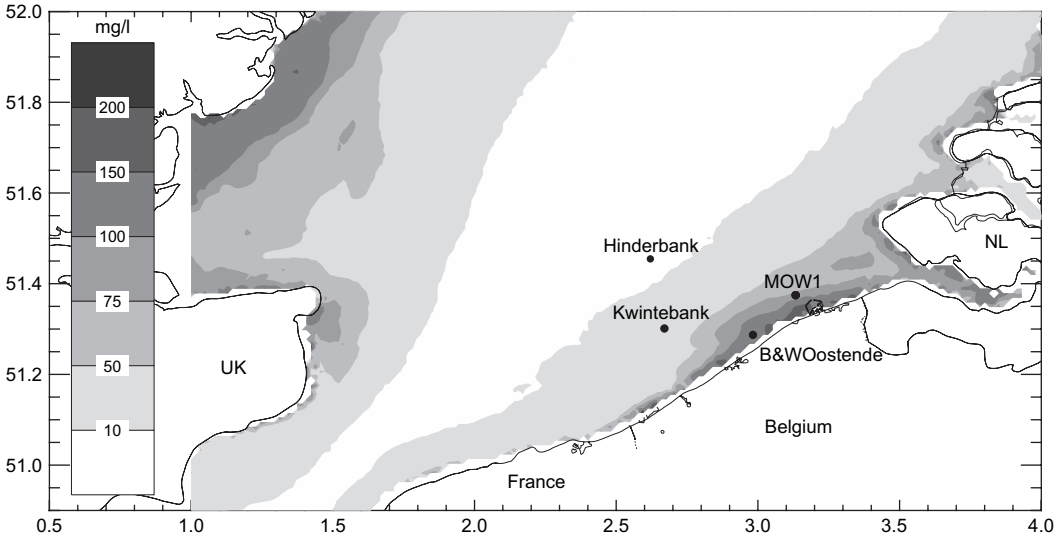

Fig. 1. Yearly averages of vertically averaged SPM concentration in the southern North Sea derived from 362 SeaWiFS images (1997–2004) (Fettweis et al., 2007b). Also shown are the locations of the tidal measurement stations. The coordinates are latitudes (°N) and longitudes (°E).

Table 1
Tidal cycle measurements, further the linear regression coefficients (±standard deviation) between the OBS signal and the SPM concentration from filtrations are shown (TM = coastal turbidity maximum)

Nr.	Date	Location	Area	SPM = $A + B \times$ OBS	
				A (±stdv)	B (±stdv)
2003/04	20–21/02/2003	B&W Oostende	TM	-7.42 ± 3.20	1.536 ± 0.026
2003/15	11–12/06/2003	Kwintebank	Offshore	1.21 ± 0.19	1.721 ± 0.010
2003/22	8–9/09/2003	MOW1	TM	10.73 ± 2.51	1.375 ± 0.080
2003/25	9–10/10/2003	Kwintebank	Offshore	7.84 ± 1.28	1.276 ± 0.068
2004/16	15–16/07/2004	B&W Oostende	TM	6.08 ± 0.85	1.537 ± 0.049
2004/25-A	8–9/11/2004	MOW1	TM	8.46 ± 2.30	1.530 ± 0.036
2004/25-B	9–10/11/2004	Hinderbank	Offshore	2.70 ± 0.36	1.422 ± 0.531
2005/15-B	21–22/06/2005	MOW1	TM	-5.91 ± 1.93	1.768 ± 0.024

A Sea-Bird SBE09 SCTD carousel sampling system (containing 12 10-l Niskin bottles) with an OBS, were kept at least 4.5 m below the surface and about 3 m above the bottom. The LISST 100C (range 2.5–500 μm) was attached directly to the carousel sampling system from March 2004 onward; before that the LISST 100C was suspended in the water at about 10 m away from the carousel. From March 2004 onward, all the data were thus collected at almost the same locations.

A Niskin bottle was closed every 20 min, thus resulting in about 40 samples per tidal cycle. The carousel was taken onboard the vessel every hour. Three sub-samples were then filtered onboard from each water sample using pre-weighed filters (Whatman GF/C). In total, 120 filtrations were thus carried out per tidal cycle. After filtration, the filters were rinsed with Milli-Q water (±50 ml) to remove the salt, dried and weighed to obtain the SPM concentration. Every hour, a fourth sub-sample was filtered onboard to analyse for particulate organic carbon (POC) and nitrogen (PON) concentration.

SPM samples were collected onboard of the vessel with a centrifuge in order to determine the median primary particle size and density. The samples were first treated with H_2O_2 and 1 N HCl to remove organic and carbonate fraction. Then the samples were rinsed with demineralised water, oven-dried at 105 °C and brought into suspension using 100 ml of demineralised water with 5 ml of peptising (mixture of $NaCO_3$ and Na-oxalate) The suspension was stirred using a magnetic stirrer and further dispersed in an ultrasonic bath. The purpose of such treatment is to break-up the aggregates into its primary constituents. The grain size analysis was carried out on the deflocculated matter using a Sedigraph 5100 for the fraction <75 μm and sieves for the coarser fraction. The total organic carbon (TOC) content was measured by weight loss after burning at 430 °C of a sample dried at 105 °C. The method applied to analyse the grain size and the instrumental accuracy is discussed in detail by Wartel et al. (1995).

2.3. Measuring instruments

2.3.1. Optical backscatter sensor (OBS)

An OBS device measures the SPM concentration. The method is based on the principle that particles reflect part of the light that is shed onto them from an external source. The amount of backscatter depends mainly on the area of the illuminated particles, but also on their shape, reflectivity, and other characteristics (e.g. Downing, 2006). At low SPM concentrations (<5-g/l mud; <50-g/l sand) and for particles with uniform diameter, the area of the illuminated particles, and therefore the backscatter, is proportional to SPM concentration.

2.3.2. LISST 100C

The LISST 100C uses laser diffraction to measure the particle size distributions in 32 logarithmically spaced size classes over the range 5–500 μm. It further incorporates a transmissometer to measure the light intensity that passes through a defined volume of water (Agrawal and Pottsmith, 2000). The volume concentration is estimated using the particle size distribution together with an empirical volume calibration constant under the assumption that the particles are spherical. Uncertainties using LISST 100C detectors may arise to non-spherical flocs, to floc sizes exceeding the instrument range, to a too high SPM concentration or to stratification of the water column (for the latter see Styles, 2006).

Agrawal and Pottsmith (2000) have shown that the LISST 100C is well suited to measure floc sizes because the diffraction patterns are formed by the flocs and aggregates themselves and not by the primary particles composing the aggregates. Multiple diffraction results in a shift towards smaller size classes and can become important when the transmission is lower than 20–30% (Agrawal and Pottsmith, 2000). Gray et al. (2004) reported errors on the data smaller than 10% if the optical transmission reduced to 10%. In the present study, only LISST 100C data with transmission higher than 20% were evaluated.

2.4. Calculation of excess density and settling velocity

By describing mud flocs with the fractal theory (Meakin, 1991; van Leussen, 1994), the floc excess density can be written as (Kranenburg, 1994):

$$\Delta\rho = \rho_f - \rho_w \propto (\rho_p - \rho_w)\left[\frac{D_f}{D_p}\right]^{nf-3} \quad (1)$$

where $\Delta\rho$ is the excess density; ρ_f, ρ_w, and ρ_p are the floc, water, and primary particle densities, respectively; D_f and D_p are the floc and primary particle sizes, respectively, and nf is the floc fractal dimension. The primary particle is defined as the first-order constituent of a floc and may consists of clay or other silicate minerals, carbonate and organic particles. D_p can, for example, be represented by the median diameter of the single grains in the flocs. Because ρ_p, ρ_w and D_p can be considered independent variables, Eq. (1) can be reduced to:

$$\Delta\rho = k_a D_f^{nf-3} \tag{2}$$

with k_a as a correlation parameter. If $\Delta\rho$ and D_f are known, then the fractal dimension can be derived using a linear regression on a log–log plot. By doing so, it is assumed that nf is constant. This assumption, however, has recently been questioned (e.g. Khelifa and Hill, 2006; Maggi, 2007; Maggi et al., 2007).

The excess floc density can be calculated if the floc and water densities are known. The water density was derived from conductivity, temperature, and pressure measurements collected by the CTD and calculated using the formulas presented in Fofonoff and Millard (1983). The floc density can be expressed as:

$$\rho_f = \frac{M_f}{V_f} \tag{3}$$

with V_f the floc volume and M_f the floc mass per unit volume. The water and primary particle mass per unit volume can be written as $M_w = \rho_w V_w$ and $M_p = \rho_p V_p$, respectively, with V_w and V_p the water and primary particle volumes in the floc. The floc density (Eq. (3)) can eventually be calculated with M_f written as:

$$M_f = M_p + M_w = M_p + \rho_w(V_f - V_p) = M_p + \rho_w\left(V_f - \frac{M_p}{\rho_p}\right) \tag{4}$$

The fall velocity, w_s, for flocs with fractal structure can be written as (Winterwerp, 1998):

$$w_s = \frac{\alpha}{18\beta}\frac{(\rho_p - \rho_w)}{\eta} g D_p^{3-nf} \frac{D_f^{nf-1}}{1 + 0.15Re^{0.687}} \tag{5}$$

where Re is the floc-Reynolds number, g is the gravitational acceleration, η is the molecular viscosity of water ($\approx 1.4 \times 10^{-3}$ kg/ms), and α and β are shape factors.

M_p was measured with an OBS and through filtration; V_f and D_f were measured with a LISST 100C. The density of primary particles, ρ_p, was calculated on the basis of the floc constituents. The density was obtained from the size distribution (using a Sedigraph) of the primary particles (D_p) and the $CaCO_3$ and total organic (TOC) contents. The fractal dimension was derived from a linear regression on a log–log plot of excess density and floc size.

2.5. Sum of errors

Based on the theory of error propagation (see e.g. chapter 14.2 in Numerical Recipes, Press et al., 1989), the standard deviation of the excess density, $\sigma_{\Delta\rho}$, can be formally written as:

$$\sigma_{\Delta\rho} = \sqrt{\left(\frac{\partial\Delta\rho}{\partial M_p}\right)^2 \sigma_{M_p}^2 + \left(\frac{\partial\Delta\rho}{\partial V_f}\right)^2 \sigma_{V_f}^2 + \left(\frac{\partial\Delta\rho}{\partial\rho_p}\right)^2 \sigma_{\rho_p}^2} \tag{6}$$

where $\Delta\rho$ is given by Eq. (1). Note that the standard deviation of the water density ρ_w is not included in the equation as the precision of water density measurements was significantly higher than that of all other parameters. Furthermore, the error in the volume concentration, V_f, is systematic and is therefore not included in the error calculation. Systematic errors are very difficult to deal with because their effects are only observable if they can be removed. One must realise that the error in V_f can be significant, as is reported in Sections 2.3.2 and 4. However, on the basis of the accuracy information provided for the LISST 100C, it is not possible to estimate this error. The standard deviation $\sigma_{\Delta\rho}$ then reduces to:

$$\sigma_{\Delta\rho} = \sqrt{\left(\frac{\partial\rho_f}{\partial M_p}\right)^2 \sigma_{M_p}^2 + \left(\frac{\partial\rho_f}{\partial\rho_p}\right)^2 \sigma_{\rho_p}^2} \tag{7}$$

with

$$\rho_f = \frac{M_f}{V_f} = \frac{M_p + \rho_w\left(V_f - \frac{M_p}{\rho_p}\right)}{V_f} = \left(1 - \frac{\rho_w}{\rho_p}\right)\frac{M_p}{V_f} + \rho_w \tag{8}$$

The standard deviation σ_{w_s} of the settling velocity w_s (Eq. (5)) is given by:

$$\sigma_{w_s} = \sqrt{\left(\frac{\partial w_s}{\partial\rho_p}\right)^2 \sigma_{\rho_p}^2 + \left(\frac{\partial w_s}{\partial D_p}\right)^2 \sigma_{D_p}^2 + \left(\frac{\partial w_s}{\partial D_f}\right)^2 \sigma_{D_f}^2 + \left(\frac{\partial w_s}{\partial nf}\right)^2 \sigma_{nf}^2} \tag{9}$$

From this (these) equation(s), it is possible to calculate the partial derivates (see Annex) and the standard deviations of the excess density and the settling velocity.

3. Results

The major sources of uncertainties are from the primary particle and floc sizes, the primary particle densities and the SPM concentration from filtration and from OBS. In the calculation of the uncertainties, only statistical errors were taken into account because we neither had enough information on systematic errors nor on errors due to a lack of measurement accuracy. This lack of accuracy cannot be treated by the statistical laws of error propagation.

3.1. Uncertainty of primary particle size

The primary particle size spectra (D_p) of the SPM were analysed on five samples using the Sedigraph 5100 (Table 2)

Table 2
Primary particles; sand, silt and clay fraction, primary particle size (D_p) ± standard deviation, TOC and $CaCO_3$ content of suspension samples collected with a centrifuge

Location	Nr.	Sand (%)	Silt (%)	Clay (%)	D_p (μm)	TOC (%)	$CaCO_3$ (%)
Kwintebank	2004/04-1	1	82	17	2.7 ± 2.5	11.6	58.2
Kwintebank	2004/04-2	–	–	–	–	6.8	38.3
Kwintebank	2004/04-3	2	63	34	1.5 ± 3.5	8.4	38.2
Kwintebank	2004/04-4	1	84	14	3.0 ± 2.3	5.0	68.7
B&W Oostende	2004/04-5	2	57	41	1.1 ± 3.7	5.1	40.3
Hinderbank	2004/05-1	–	–	–	–	7.2	55.1
Hinderbank	2004/05-2	19	71	11	7.2 ± 3.0	6.8	54.4
Kwintebank	2004/08	–	–	–	–	7.5	52.0
B&W Oostende	2004/05	–	–	–	–	9.1	33.9

after removal of organic matter and $CaCO_3$ (Fig. 2). The mean particle sizes per location were 7.2 ± 3.0 μm on the Hinderbank (offshore), 2.1 ± 1.5 μm on the Kwintebank (at the edge of the turbidity maximum), and 1.1 ± 3.7 μm in the turbidity maximum (near Oostende). The measurements suggest that the primary particle size increases towards the offshore. Wartel et al. (1995) concluded that for the Sedigraph the relative error on the concentration of particles in the separate fractions is lower than 0.7%. The error can therefore mainly be attributed to the calculation of the mean size. The primary particle sizes are valid only for the silicate fraction, as $CaCO_3$ and TOC have been eliminated before analysis. The carbonate fraction in the SPM is important but it is not yet clear how much of if it resides in the flocs and how much is of planktonic origin.

3.2. Uncertainty of primary particle density

The averages of TOC, $CaCO_3$ and silicate (>80% clay and silt) contents in the SPM from the offshore area (Kwintebank and Hinderbank) were 7.6%, 52.1% and 40.3%, respectively, and from the coastal turbidity maximum area (Oostende) 7.1%, 37.1% and 55.9%, respectively. We do not have sufficient data (seven for Kwintebank and Hinderbank, two for Oostende)

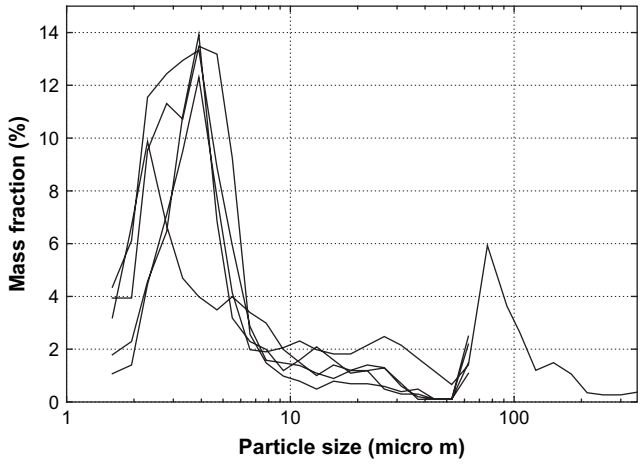

Fig. 2. Primary particle size distribution of the SPM measured with a Sedigraph 5100 and by sieving. The rising tail at 62.5 μm in four out of the five spectra includes the sand fraction without further detail. Note that in one spectrum (2004/05-2, Hinderbank) two grain size populations are present.

to meaningfully assess statistical uncertainties. The fact that the results indicate higher TOC and $CaCO_3$ contents further offshore, and a higher silicate fraction in the turbidity maximum area, should therefore be considered with some caution. The TOC, $CaCO_3$ and silicate fraction in the SPM corresponded to the total particulate matter in suspension at the time of sampling and may thus include matter that is not part of the flocs, such as plankton. The density of the primary particles has been calculated as the weighted sum of the density of the silicate, carbonate, and organic fractions. The mineral composition of clay in the SPM is on average 54% illite, 22% smectite and 24% kaolinite (Fettweis et al., 2006). The density of these clay minerals varies and situated between 2300 and 2700 kg/m^3, while the density of the other minerals (carbonate and quartz) is between 2600 and 2800 kg/m^3, and that of the organic matter between 900 and 1300 kg/m^3 (Pilatti et al., 2006). It was not possible to accurately calculate the density of the particulate matter in the SPM on the basis of the given information and was thus estimated from the weighted average of the silicate, $CaCO_3$ and TOC fractions as 2498 ± 197 kg/m^3 (offshore) and 2475 ± 217 kg/m^3 (coastal turbidity maximum).

3.3. Uncertainty of SPM concentration

The SPM concentration was measured by OBS and filtration of sea water. The best way to calibrate an OBS is to take water samples immediately adjacent to the sensor and to draw a calibration curve between the signal and the SPM concentration (Sternberg et al., 1991) (see Fig. 3 and Table 1).

3.4. Uncertainty of floc size

The particle size distributions measured with the LISST 100C during individual tidal cycles are illustrated in Fig. 4. These data show that a rising tail occurs in the largest size classes in six of the eight tidal cycles. Maxima in the smallest size class occur in three tidal cycles. If the maxima in the smallest and largest size class are not related to the actual size distribution, then the calculation of the average floc size, volume concentration, and standard deviation will be uncertain. The mean floc size and the standard deviation can be calculated from the particle sizes spectra of the LISST using the methods of moments (Folk, 1966). The average of all mean floc sizes and standard deviations per tidal cycle is given in Table 3. From the 2003/04 cycle only eight (of the 700) LISST data have a transmission higher than 20%, thus indicating that the results of this campaign should be viewed with caution.

3.5. Uncertainty of excess density, fractal dimension and settling velocity

The excess density and the settling velocity have been calculated as described in Section 2.4. The sum of errors has been derived following Eqs. (6) and (9). The results for excess density and fractal dimension are presented in Table 3 and Fig. 5. The averages of the excess density over the measurement cycle indicate that the excess density of the flocs is

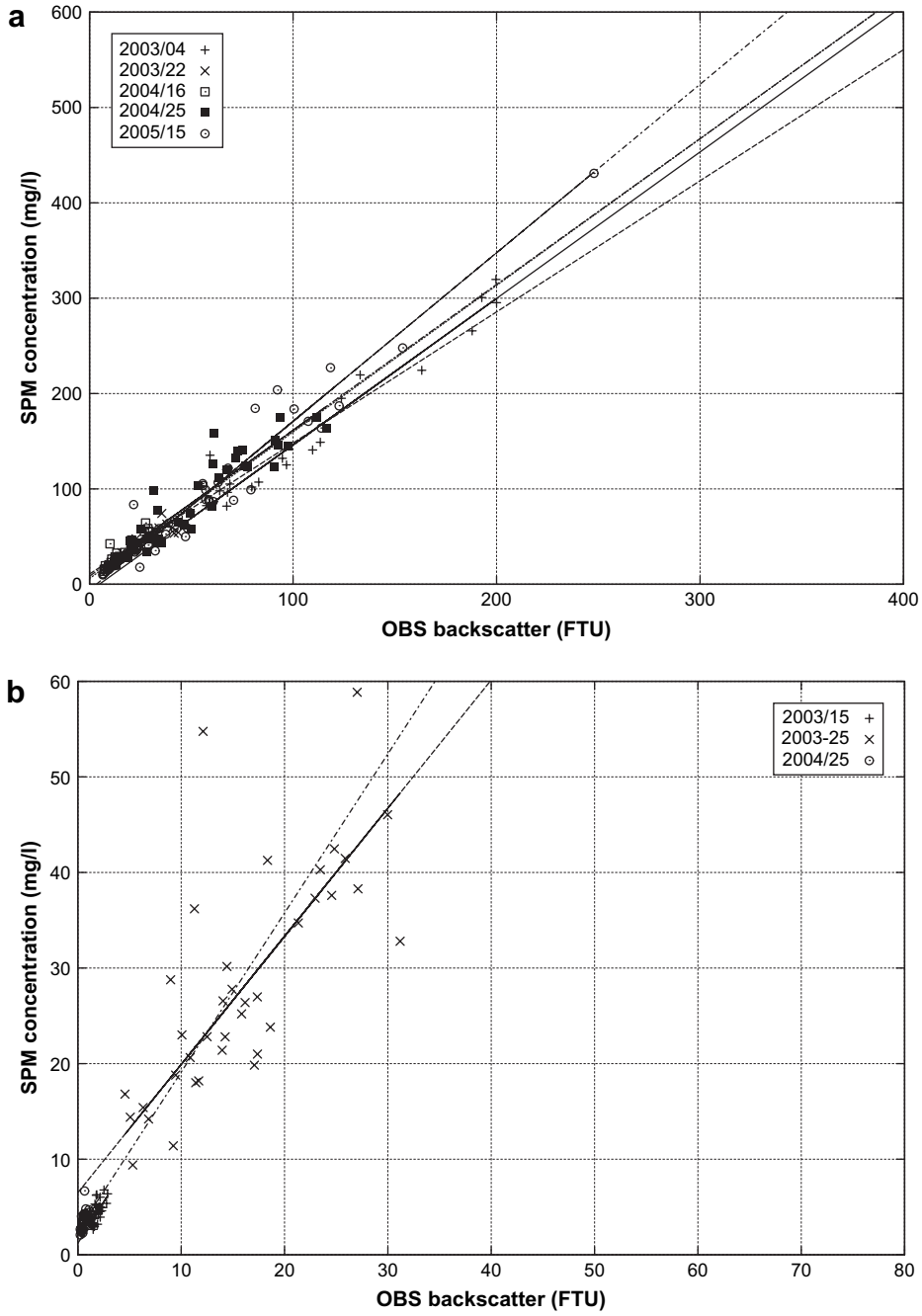

Fig. 3. OBS signal vs. SPM concentration with regression lines calculated to calibrate the OBS for the measurements at (a) MOW1 and B&W Oostende (turbidity maximum) and (b) Kwintebank and Hinderbank (offshore zone).

situated between 117 and 906 kg/m^3. In the literature, by comparison, values for the excess density of about 50 kg/m^3 (or lower) up to 300 kg/m^3 have been reported (e.g. Winterwerp, 1998). The fractal dimensions are between 1.46 and 2.19; typical values reported in the literature are between 1.7 and 2.25 (Lick et al., 1993; Ten Brinke and Dronkers, 1993; Kranenburg, 1994; Winterwerp et al., 2006). The averages of the settling velocities over the measurement period (only data with nf < 3) are between 0.003 and 0.20 mm/s, and are of the same order of magnitude as values reported in the literature (van Leussen, 1994; Fugate and Friederichs, 2003; Winterwerp et al., 2006) (see Fig. 5). The standard deviations for ρ, nf and w_s are presented as averages over each measurement cycle in Table 3. The relative standard deviations for ρ, nf and w_s over all the measurements are about 10%, 2.5% and 100%, respectively.

4. Discussion

The calculated uncertainty of the excess density and settling velocity should be regarded as lower limits of the real error because the systematic errors, which are due to a lack of accuracy of the measuring instruments (mainly LISST, OBS and Sedigraph), have been omitted. It is

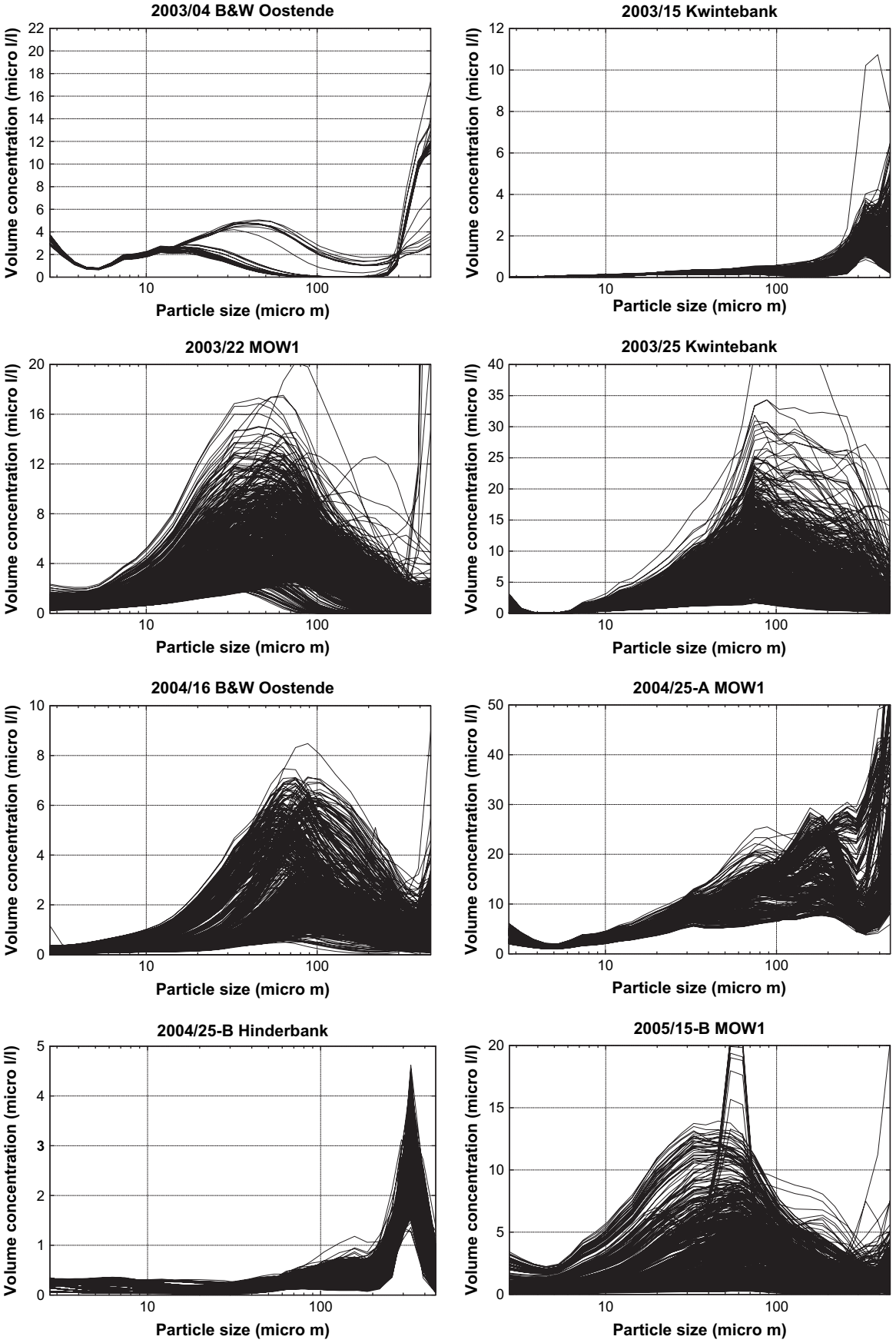

Fig. 4. Particle (floc) size distribution of the SPM measured by the LISST as a function of volume concentration. Note that only the distributions with a transmission greater then 20% are shown.

Table 3
Tidal averages of SPM concentration from filtration (mg/l), floc size D_f (μm), excess density $\Delta\rho$ (kg/m^3), fractal dimension nf and settling velocity (mm/s), also indicated is the standard deviation. The fractal dimension has been obtained from a linear regression of all data per tidal cycle on a log–log plot. Remark that nf (and thus also w_s) is unrealistic (>3) in three campaigns

Nr.	SPM ± stdv	D_f ± stdv	$\Delta\rho$ ± stdv	nf ± stdv	w_s ± stdv
2003/04	281 ± 224	52 ± 23	706 ± 58	3.02 ± 0.21	1.45 ± 1.29
2003/15	4.5 ± 1.1	160 ± 38	226 ± 16	2.06 ± 0.02	0.20 ± 0.14
2003/22	48 ± 22	44 ± 14	451 ± 42	1.46 ± 0.05	0.003 ± 0.015
2003/25	27 ± 12	75 ± 20	160 ± 14	2.08 ± 0.04	0.09 ± 0.07
2004/16	32 ± 14	81 ± 22	600 ± 49	3.23 ± 0.06	8.43 ± 8.27
2004/25-A	89 ± 54	88 ± 25	117 ± 10	1.72 ± 0.03	0.01 ± 0.05
2004/25-B	3.6 ± 1.3	115 ± 34	161 ± 21	3.25 ± 0.03	12.27 ± 8.30
2005/15-B	104 ± 89	62 ± 19	906 ± 77	2.19 ± 0.04	0.07 ± 0.18

important to note that we are dealing with errors in the sense that measurements have been carried out with a lack of precision for the SPM concentrations from filtration and thus the calibration of the OBS and (partly) the primary particle density. The particle size measurements with LISST or Sedigraph also suffer from a lack of precision, but this has not been taken into account. The uncertainties in this case are mainly associated with the fact that the primary particle and floc sizes are introduced in Eqs. (3) and (5) as single values, although in nature they actually represent a spectrum of sizes. If we replace this natural variation in particle sizes by one value, then a typical statistical error is introduced, which has here been represented by the standard deviation, i.e., the limits between which 67% of the values are situated. The fact that the error in the fall velocity is very high, even without taking into account systematic errors of the measuring instruments or the sampling methods, is therefore not surprising.

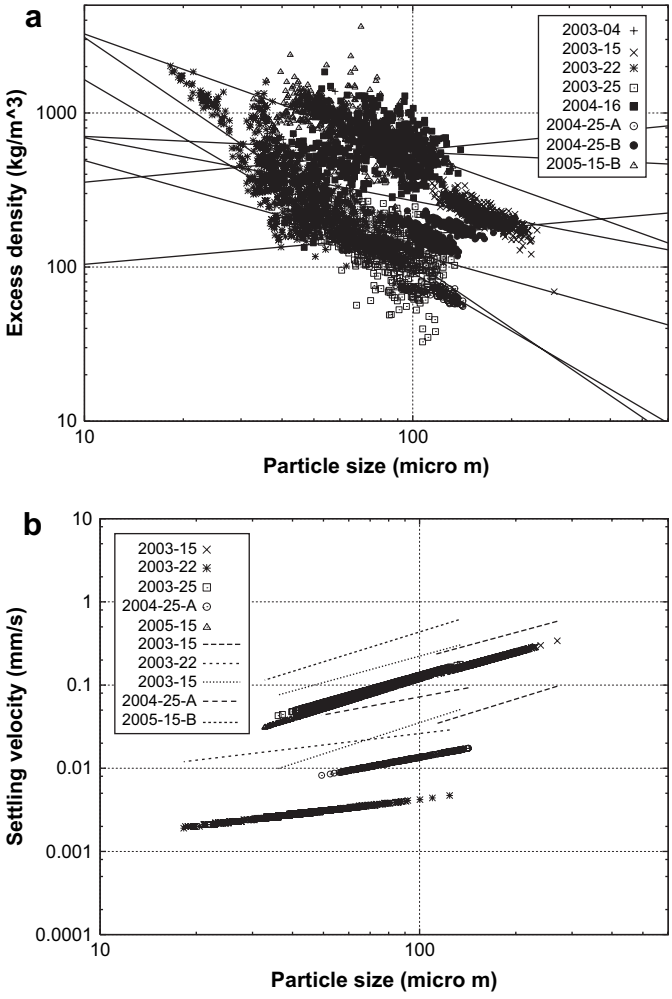

Fig. 5. (a) Excess density (calculated with Eq. (1)) as a function of floc size. Also shown are the regression lines for every measurement cycle. (b) Settling velocity as a function of floc size calculated with the modified Stokes' Law (Eq. (5)) and using a constant fractal dimension per measurement cycle; only cycles with nf < 3 are shown. The lines represent $w_s \pm$ standard deviation (if w_s – standard deviation < 0, then the line is not shown).

4.1. Origin of the errors

The results show that the origin of the error in the settling velocity is mainly due to uncertainties in the primary particle size D_p and the floc size D_f. These results are complementary to those of Khelifa and Hill (2006) who have underlined the dominant effect which primary particle size has on the excess density and thus on the settling velocity. The results from the error analysis have shown that the statistical uncertainties in the settling velocity will always be high when dealing with natural flocs or particles, and that they cannot be reduced by increasing the accuracy of the instruments, the measuring procedure, or the method of calculating the settling velocity. In other words, they are always the dominating ones. These actions will, however, increase the reliability of the settling velocity measurements – in the sense that the value corresponds better with reality – as systematic errors are reduced or precision is increased.

A higher reliability in the results was obtained from March 2004 onwards due to a change in the measuring configuration: from that date onward, the LISST 100C was directly attached to the carousel sampling system whereas before it was suspended from a cable located about 10 m away from the carousel. The LISST 100C data were then acquired at virtually the same location as the water samples, the OBS, and the CTD data. A higher reliability can also be obtained by using a model, which is not based on the assumption of self-similarity of natural flocs and thus does not assume a constant fractal dimension during a tidal cycle (see e.g. Khelifa and Hill, 2006).

Not enough data have yet been collected to understand how the primary particle sizes vary in time and space, and thus to know how much precision is lost if values of D_p measured at a different time than the tidal measurements are used in the calculation of the excess density. In the southern North Sea, different sources of mud exist (Fettweis et al., 2007a), and this could lead to different characteristics of the size, density and composition of primary particles, depending on meteorological (wind direction, wave height) and river runoff conditions.

The origin of the error in the excess density is due to uncertainties in the SPM concentration (M_p) and the density of the primary particles, except for the offshore measurements where uncertainties in the SPM concentration (M_p) dominate. The magnitude of the error is relatively small (10%). This, however,

does not mean that the excess density values are reliable. The variability in the densities of the heterogeneous primary particles, the statistical nature of primary particle distributions, and the fact that probably not all the organic matter is in the floc, make the determination of excess density particularly problematical. Wolanski et al. (2003), for example, have compared the mineral fraction with ballast that regulates the buoyancy and thus the settling velocity of marine snow.

4.2. Floc size

When interpreting the results of the LISST, one should take into account that the average particle size is frequently an under − or overestimate of the real value because particles outside the range of the instrument are pooled in the smallest and/or largest size classes ('rising tails') and because the instrument underestimates the size of mono-sized particles by 10% (Gartner et al., 2001) and thus also underestimates the volume concentration. These errors are not statistical, but of systematic nature, and reflect the lack of accuracy of the instruments. Mikkelsen et al. (2005) propose to reduce the influence of a rising tail in the spectrum by omitting the smallest and largest size classes when calculating the average floc size. However, in this case the data do not include the whole particle size spectrum and thus possibly misses important parts of the spectrum. Furthermore, the floc size is then only valid for a part of the size spectrum, whereas the mass of particles in the flocs (M_p) is determined for the whole suspended matter. In addition, the values obtained for excess density and fall velocity are then possibly also less realistic. However, the order of magnitude of the error remains the same.

Another uncertainty in floc size distribution measured by the LISST 100C is due to the fact that natural particles (flocs) are slightly flattened because of the complex associations of lithogenic and organic constituents (van Leussen, 1994). Mikkelsen and Pejrup (2001) argue that the influence of a slight flattening seems to be negligible on particle size distribution and volume concentration measured by a laser diffraction instrument. Pedocchi and Garcia (2006), however, report that the scattered light pattern of natural particles might be significantly different from that of spheres. Our data show that averages of the excess density were lower in the offshore (181 kg/m^3) than in the turbidity maximum (548 kg/m^3) area. This pattern correlates with the average higher flocs sizes (117 μm vs. 66 μm) and smaller settling velocities (0.14 mm/s vs. 0.29 mm/s) in the offshore area. The differences in floc size, excess density, and settling velocity between a low ('offshore') and a high turbidity site has partly been ascribed to the higher availability of organic matter (represented by the ratio of POC concentration over SPM concentration) at the low turbidity sites (Fettweis et al., 2006). The relatively higher availability of organic matter offshore, and the fact that aggregates with a higher organic matter content have a more irregular shape, could indicate that the LISST 100 measurements have a lower (at least different) precision at the low turbidity sites than measurements in turbidity maxima having relatively lower organic matter concentrations and probably more regular aggregate shapes.

4.3. SPM concentration

The mass of primary particles per unit volume has been equated with SPM concentration measured by the OBS after calibration with results of the filtration of in situ water samples. Since the output of an OBS is proportional to the volume concentration and inversely proportional to the particle diameter this dependence between the output of the OBS and the total suspended matter concentration is therefore not uniform if the particle size changes as a function of time, as frequently observed in coastal zones and estuaries (Fugate and Friederichs, 2002). Downing (2006) mentions that the primary factors causing the OBS signal to change are in decreasing order of importance with respect to the SPM concentration, particle size, and particle shape. Another source of uncertainties of the OBS is due to the calibration using water samples. Uncertainties from filtration of water samples arise due to bad homogenization of the sample, the filtration method, and the precision in measuring the filtration volume with a beaker (2 mg/l for filtration volume < 250 ml). At every sampling occasion, three sub-samples were taken for filtration (see Section 2.2). In 19% of the samples the relative standard deviation between the three sub-samples was higher than 6%, the value increasing with decreasing SPM concentration. The lack of precision in the high SPM concentration samples is most probably due to bad homogenization of the sample, whereas for the low SPM concentration samples it is most probably due to the filtration method, as described by Van Mol et al. (2006). They have compared the method presented in Section 2.2 with another one where finer filters (Whatman GF/F) and a more elaborate rinsing method for the elimination of the salt was used. Their conclusion was that our method on average gives a 4.5 mg/l higher SPM concentration, which would mean that with our filtration method a systematic error of at most 4.5 mg/l is introduced. This is mainly of significance for the low SPM concentration measurements, as in cycles 2003/15 and 2004/25-A. The SPM concentration obtained through filtration is about 5 mg/l (see Table 3); a systematic error of the same order of magnitude as the measured value results in a significantly different excess density and fall velocity. Moreover, the fact that the SPM concentration stays nearly constant during these measurements, results in a less precise calculation of the regression line in Fig. 3, especially for cycle 2004/25-A, and thus of the SPM concentration from the OBS.

5. Conclusions

The settling of mud flocs has a major influence on the transport of cohesive sediments; it is furthermore an important parameter in sediment transport models. Measurements of settling velocity are inherently associated with uncertainties due to a lack of accuracy of the measuring instruments and due to the statistical nature of particle size distributions (and excess densities) in the suspended matter. These errors occur when using both direct or indirect methods to obtain settling velocities. A comprehensive analysis of uncertainties of an

indirect method to calculate settling velocity has been presented and the conclusions are as follows.

(1) The relative standard deviation in settling velocity due to statistical uncertainties is at least 100%. The error mainly derives from uncertainties of the primary particle and the floc sizes, respectively. These statistical uncertainties will always be high when dealing with natural flocs or particles and cannot be reduced by increasing the accuracy of the instruments.
(2) The statistical error on the excess density is mainly due to uncertainties in the SPM concentration and in the primary particle density.
(3) More reliable values of settling velocity can, for example, be obtained by increasing the precision of the measurements, the accuracy of the instruments, and not assuming self-similarity of floc structures.
(4) It is crucial to have data on primary particle size and density at the same moment as floc size and SPM concentration are measured, as these parameters are of major importance in calculating the excess density and the settling velocity. Measurements of suspended matter should include an analysis of its major constituents (organic matter, $CaCO_3$ and silicate minerals) and the grain size.

An important part of our understanding of flocculation and cohesive sediment dynamics (deposition and erosion) is based on measurements. The uncertainties associated with indirect (or direct) settling velocity measurements are very high due to their statistical nature; the total error will be even higher because systematic errors due to a lack of accuracy of the measuring instruments are not included. Our results underline that the statistical nature of flocculation processes and settling velocity must be taken into account when modelling cohesive sediment transport, i.e., by at least one standard deviation of settling velocity based on measurements, or by introducing a floc size (and settling velocity) distribution in the transport model.

Acknowledgements

This study was partly funded by the Maritime Access Division of the Ministry of the Flemish Community in the framework of the MOMO project and partly by the Belgian Science Policy within the framework of the QUEST4D project. The measurements have been collected onboard of the R/V Belgica. The author is grateful to F. Maggi (University of California, Berkeley) and S. Legrand (MUMM) for their constructive suggestions and to J.-P. De Blauwe, J. Backers, F. Francken and D. Van den Eynde (MUMM) for their help in collecting and compiling the measurement data.

Annex

The partial derivatives in Eq. (7) are given by:

$$\frac{\partial \rho_f}{\partial M_p} = \frac{1}{V_f}\left(1 - \frac{\rho_w}{\rho_p}\right) \tag{A.1}$$

$$\frac{\partial \rho_f}{\partial \rho_p} = \frac{\rho_w M_p}{\rho_p^2 V_f} \tag{A.2}$$

and for the standard deviation, $\sigma_{\Delta\rho}$, of the excess density one gets eventually:

$$\sigma_{\Delta\rho} = \frac{1}{V_f}\sqrt{\left(1 - \frac{\rho_w}{\rho_p}\right)^2 \sigma_{M_p}^2 + \frac{\rho_w^2 M_p^2}{\rho_p^4}\sigma_{\rho_p}^2} \tag{A.3}$$

The partial derivatives in Eq. (9) are given by:

$$\frac{\partial w_s}{\partial \rho_p} = \frac{\alpha g}{18\beta\eta} D_p^{3-nf} \frac{D_f^{nf-1}}{1 + 0.15Re^{0.687}} \tag{A.4}$$

$$\frac{\partial w_s}{\partial D_p} = \frac{\alpha g\left(\rho_p - \rho_w\right)}{18\beta\eta}(3 - nf) D_p^{2-nf} \frac{D_f^{nf-1}}{1 + 0.15Re^{0.687}} \tag{A.5}$$

$$\frac{\partial w_s}{\partial D_f} = \frac{\alpha g\left(\rho_p - \rho_w\right)}{18\beta\eta}(nf - 1) D_p^{3-nf} \frac{D_f^{nf-2}}{1 + 0.15Re^{0.687}} \tag{A.6}$$

$$\frac{\partial w_s}{\partial nf} = \frac{\alpha g\left(\rho_p - \rho_w\right)}{18\beta\eta} D_p^{3-nf} \frac{D_f^{nf-1}}{1 + 0.15Re^{0.687}} \ln D_f \tag{A.7}$$

and the standard deviation, σ_{w_s}, of the settling velocity then is:

$$\sigma_{w_s} = aD_p^{3-nf} D_f^{nf-1} \times \sqrt{\sigma_{\rho_p}^2 + \left(\rho_p - \rho_w\right)^2 \left[\frac{(3-nf)^2}{D_p^2}\sigma_{D_p}^2 + \frac{(nf-1)^2}{D_f^2}\sigma_{D_f}^2 + \left(\ln D_f\right)^2 \sigma_{nf}^2\right]} \tag{A.8}$$

with

$$a = \frac{\alpha g}{18\beta\eta} \frac{1}{1 + 0.15Re^{0.687}} \tag{A.9}$$

References

Agrawal, Y.C., Pottsmith, H.C., 2000. Instruments for particle size and settling velocity observations in sediment transport. Marine Geology 168, 89–114.

Chang, T.S., Joerdel, O., Flemming, B.W., Bartholomä, A., 2006. The role of particle aggregation/disaggregation in muddy sediment dynamics and seasonal sediment turnover in a back-barrier tidal basin, East Frisian Wadden Sea, southern North Sea. Marine Geology 235, 49–61.

Curran, K.J., Hill, P.S., Milligan, T.G., Mikkelsen, O.A., Law, B.A., Durrieu de Madron, X., Bourrin, F., 2007. Settling velocity, effective density, and mass composition of suspended sediment in a coastal bottom boundary layer, Gulf of Lions, France. Continental Shelf Research 27, 1408–1421.

Downing, J., 2006. Twenty-five years with OBS sensors: The good, the bad, and the ugly. Continental Shelf Research 26, 2299–2318.

Dyer, K.R., Cornelisse, J., Dearnaley, M.P., Fennessy, M.J., Jones, S.E., Kappenberg, J., McCave, I.N., Pejrup, M., Puls, W., van Leussen, W., Wolfstein, K., 1996. A comparison on *in situ* techniques for estuarine floc settling velocity measurements. Journal of Sea Research 36, 15–29.

Eisma, D., Kalf, J., 1987. Distribution, organic content and particle size of suspended matter in the North Sea. Netherlands Journal of Sea Research 21, 265–285.

Eisma, D., Bale, A.J., Dearnaley, M.P., Fennessy, M.J., van Leussen, W., Maldiney, M.-A., Pfeiffer, A., Wells, J.T., 1996. Intercomparison of *in*

situ suspended matter (floc) size measurements. Journal of Sea Research 36, 3–14.

Fettweis, M., Francken, F., Pison, V., Van den Eynde, D., 2006. Suspended particulate matter dynamics and aggregate sizes in a high turbidity area. Marine Geology 235, 63–74.

Fettweis, M., Du Four, I., Zeelmaekers, E., Baeteman, C., Francken, F., Houziaux, J.-S., Mathys, M., Nechad, B., Pison, V., Vandenberghe, N., Van den Eynde, D., Van Lancker, V., Wartel, S., 2007a. Mud Origin, Characterisation and Human Activities (MOCHA). Final Scientific Report. Belgian Science Policy, Brussels, 59 pp.

Fettweis, M., Nechad, B., Van den Eynde, D., 2007b. An estimate of the suspended particulate matter (SPM) transport in the southern North Sea using SeaWiFS images, in situ measurements and numerical model results. Continental Shelf Research 27, 1568–1583.

Fofonoff, N.P., Millard, R.C., 1983. Algorithms for Computation of Fundamental Properties of Seawater. UNESCO Technical Papers in Marine Science, 44. UNESCO Division of Marine Science, Paris, 53 pp.

Folk, R.L., 1966. A review of grain-size parameters. Sedimentology 6, 73–93.

Fugate, D.C., Friederichs, C.T., 2002. Determining concentration and fall velocity of estuarine particle populations using ADV, OBS and LISST. Continental Shelf Research 22, 1867–1886.

Fugate, D.C., Friederichs, C.T., 2003. Controls on suspended aggregate size in partially mixed estuaries. Estuarine, Coastal and Shelf Science 58, 389–404.

Gartner, J.W., Cheng, R.T., Wang, P.F., Richter, K., 2001. Laboratory and field evaluations of the LISST-100 instrument for suspended particle size distributions. Marine Geology 175, 199–219.

Gray, J.R., Agrawal, Y.C., Pottsmith, H.C., 2004. The LISST-SL streamlined isokinetic suspended-sediment profiler. In: Cheng, L. (Ed.), Proceedings of the 9th International Symposium River Sedimentation. China.

Jackson, G.A., 2005. Coagulation theory and models of oceanic plankton aggregation. In: Droppo, I., Leppard, G., Liss, S., Milligan, T. (Eds.), Flocculation in Natural and Engineered Environmental Systems. CRC Press, pp. 271–292.

Khelifa, A., Hill, P.S., 2006. Models for effective density and settling velocity of flocs. Journal of Hydraulic Research 44, 390–401.

Kranenburg, C., 1994. On the fractal structure of cohesive sediment aggregates. Estuarine, Coastal and Shelf Science 39, 451–460.

Lee, K., Matsoukas, T., 2000. Simultaneous coagulation and break-up using constant-N Monte Carlo. Powder Technology 110, 82–89.

Lick, W., Huang, H., Jepsen, R., 1993. Flocculation of fine-grained sediments due to differential settling. Journal of Geophysical Research 98 (C6), 10279–10288.

van Leussen, W., 1994. Estuarine Macroflocs and their Role in Fine-grained Sediment Transport. Ph. D. thesis, University of Utrecht, The Netherlands.

Maggi, F., 2007. Variable fractal dimension: a major control for floc structure and flocculation kinematics of suspended cohesive sediments. Journal of Geophysical Research 112, C07012.

Maggi, F., Mietta, F., Winterwerp, J.C., 2007. Effect of variable fractal dimension on the floc size distribution of suspended cohesive sediment. Journal of Hydrology 343, 43–55.

Meakin, P., 1991. Fractal aggregates in geophysics. Reviews of Geophysics 29, 317–354.

Mikkelsen, O.A., Pejrup, M., 2001. The use of a LISST-100 laser particle sizer for in-situ estimates of floc size, density and settling velocity. Geo-Marine Letters 20, 187–195.

Mikkelsen, O.A., Hill, P.S., Milligan, T.G., Chant, R.J., 2005. In situ particle size distribution and volume concentrations from a LISST-100 laser particle sizer and a digital floc camera. Continental Shelf Research 25, 1959–1978.

Pedocchi, F., Garcia, M.H., 2006. Evaluation of the LISST-ST instrument for suspended particle size distribution and settling velocity measurements. Continental Shelf Research 26, 943–958.

Pilatti, M.A., Ghiberto, P.J., Imhoff, S., 2006. Application of a general relationship between soil particle density and organic matter to mollisols of Santa Fe (Argentina). In: 18th World Congress of Soil Science, USA.

Press, W.H., Flannery, B.P., Teukolsky, S.A., Vetterling, W.T., 1989. Numerical Recipes: The Art of Scientific Computing (Fortran Version). Press Syndicate of the University of Cambridge, 702 pp.

Sternberg, R.W., Kineke, G.C., Johnson, R.V., 1991. An instrument system for profiling suspended sediment, fluid, and flow conditions in shallow marine environments. Continental Shelf Research 11, 109–122.

Styles, R., 2006. Laboratory evaluation of the LISST in a stratified fluid. Marine Geology 227, 151–162.

Ten Brinke, W.B.M., Dronkers, J., 1993. Physical and biotic aspects of fine-sediment import in the Oosterschelde tidal basin (The Netherlands). Netherlands Journal of Sea Research 31, 19–36.

Van Mol, B., Knockaert, M., Saudemont, D., Roose, P., Ruddick, K., 2006. Suspended Particulate Matter Filtration Test. MUMM Report, Brussels.

Wartel, S., Barusseau, J.-P., Cornand, L., 1995. Improvement of grain-size analyses using the automated SEDIGRAPH 5100. Studiedocumenten van het K.B.I.N. – Documents de travail de l'I.R.Sc.N.B., Brussels.

Winterwerp, J., 1998. A simple model for turbulence induced flocculation of cohesive sediments. Journal of Hydraulic Research 36, 309–326.

Winterwerp, J., Manning, A.J., Martens, C., De Mulder, T., Vanlede, J., 2006. A heuristic formula for turbulence-induced flocculation of cohesive sediment. Estuarine, Coastal and Shelf Science 68, 195–207.

Wolanski, E., Richmond, R.H., Davis, G., Bonito, V., 2003. Water and fine sediment dynamics in transient river plumes in a small, reef-fringed bay, Guam. Estuarine, Coastal and Shelf Science 56, 1029–1043.